

Optimized surface-enhanced Raman scattering on gold nanoparticle arrays

N. Féridj, J. Aubard, G. Lévi, J. R. Krenn, A. Hohenau et al.

Citation: *Appl. Phys. Lett.* **82**, 3095 (2003); doi: 10.1063/1.1571979

View online: <http://dx.doi.org/10.1063/1.1571979>

View Table of Contents: <http://apl.aip.org/resource/1/APPLAB/v82/i18>

Published by the [AIP Publishing LLC](#).

Additional information on *Appl. Phys. Lett.*

Journal Homepage: <http://apl.aip.org/>

Journal Information: http://apl.aip.org/about/about_the_journal

Top downloads: http://apl.aip.org/features/most_downloaded

Information for Authors: <http://apl.aip.org/authors>



Optimized surface-enhanced Raman scattering on gold nanoparticle arrays

N. Félidj, J. Aubard, and G. Lévi^{a)}

Interfaces, Traitements, Organisation et Dynamique des Systèmes-CNRS UMR 7086 1, rue Guy de la Brosse 75005 Paris, France

J. R. Krenn, A. Hohenau, G. Schider, A. Leitner, and F. R. Aussenegg

Institut für Experimentalphysik, Universität Karl Franzens, Universitätplatz 5, A-8010 Graz, Austria

(Received 17 December 2002; accepted 10 March 2003)

In this letter, we show that tuning the maximum of the surface plasmon resonance of elongated gold nanoparticles to a wavelength, the position of which is precisely midway between the exciting laser line and the Raman line, results in an optimization of the surface-enhanced Raman-scattering effect.

© 2003 American Institute of Physics. [DOI: 10.1063/1.1571979]

Surface-enhanced Raman scattering (SERS) is a very sensitive spectroscopy that allows the detection of organic molecules adsorbed on noble metal substrates (silver, gold, copper) at submicromolar concentration.^{1,2} A wide variety of substrates has been found to exhibit SERS: electrochemically modified electrodes,³ colloids,⁴ island films,⁵⁻⁷ particles grafted on silanized glasses,⁸ and more recently regular particle arrays.^{9,10} Two mechanisms have been considered to explain the SERS effect. The main contribution arises from a huge enhancement of the local electromagnetic field close to surface roughness, due to the excitation of a localized surface plasmon (LSP),^{1,2,11} while a further enhancement can be observed for molecules adsorbed onto specific sites when resonant charge transfer occurs.¹²

Optimization of the Raman amplification is of paramount interest for applying the SERS technique in biosensors for single molecule detection,^{13,14} or for optical sensors in nanoscale integrated devices. This optimization is a great challenge that requires finding out the connection existing between the LSP resonance wavelength and the Raman enhancement factor. The very few studies devoted to the determination of such a correlation,^{6,15,16} were made difficult by the broad size and shape distributions of the particles constituting the substrate,^{4,5,8,15} resulting in an inhomogeneous broadening that blurred the LSP resonance.

In this letter, we show that the use of regular particle arrays with nanometer scale structures can give rise to an optimized SERS spectrum of a molecular probe adsorbed at quite low concentration. Thanks to their very narrow particle distribution, these arrays exhibit very sharp LSP resonances leading us to demonstrate experimentally the required condition for this optimization. This condition is to choose the particle size and shape such that the corresponding plasmon wavelength is suitably located between the wavelength of the laser excitation and that of the Raman band under consideration, at equal distance from one to the other. Particle arrays are produced by thermal evaporation of gold following electron-beam lithography on a modified JEOL 6400 scanning electronic microscope.^{17,18} This technique enables us to control the particle size, shape, and spacing and to locate the plasmon resonance at almost any desired visible wavelength.

Let us first consider the extinction spectrum of a regular array of elongated gold particles deposited on an indium tin oxide ITO-doped glass substrate that displays two bands (Fig. 1) corresponding to LSPs polarized along the two-particle principal axes parallel to the substrate.^{19,20} The first one located at 647 nm is polarized along the medium axis (*transverse polarization*) while the second one at 846 nm is polarized along the major axis (*longitudinal polarization*). Raman spectra of trans-1,2-bi-(4-pyridyl) ethylene (BPE) were recorded on a Jobin-Yvon T64000 microspectrometer by focusing the laser line on the array immersed into a 5×10^{-4} M BPE aqueous solution.¹⁰ The investigated spectral region was limited from 1500 to 1700 cm^{-1} , where the BPE molecule displays its major Raman bands. For an excitation at 647 nm (Kr^+ laser line), under a polarization along the medium particle axis, the transverse plasmon resonance is excited and a huge SERS spectrum is observed (Fig. 2, spectrum A). This result is in agreement with the often-

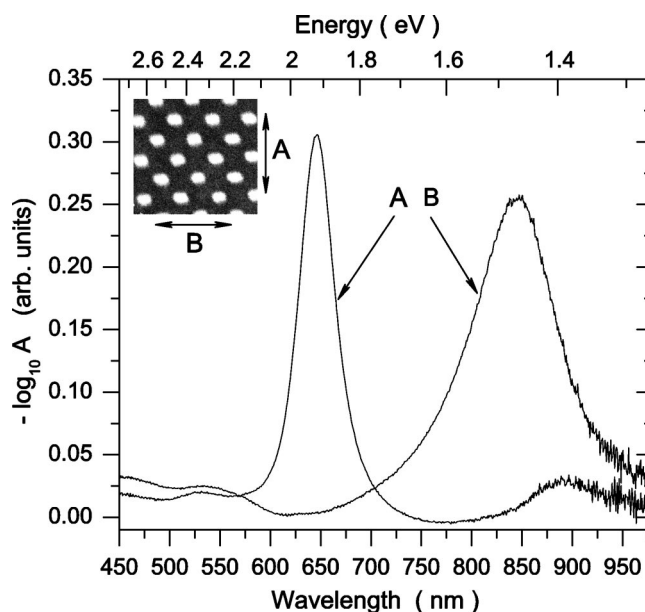


FIG. 1. Extinction spectrum of a regular array of gold elongated nanoparticles; major and medium axes of 175 and 126 nm, respectively, are parallel to the substrate (particle aspect ratio $r = 1.39$), particle height is 40 nm, and the spacing between particles is $\Lambda = 461$ nm. The spectrum is acquired by transmission under normal incidence in water; "A" denotes the transverse polarization and "B" the longitudinal one. Inset: scanning electronic image of the array (detail).

^{a)}Electronic mail: levi@paris7.jussieu.fr

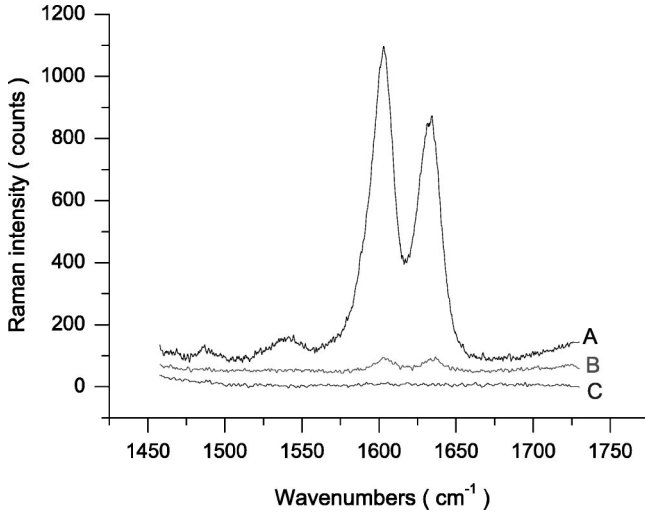


FIG. 2. SERS spectra of a 5×10^{-4} M BPE aqueous solution for the array shown in the inset of Fig. 1. Spectra A and B correspond to laser excitation along the transverse (A) and longitudinal (B) LSP resonances, respectively; spectrum C is recorded out of the array. Spectra A, B, and C were recorded under identical experimental conditions: laser excitation 647 nm; power 15 mW at the sample, slit width $300 \mu\text{m}$; three accumulations of 180 s counting time each. The spectra are vertically shifted for clarity.

encountered expression for the Raman gain:^{2,16}

$$G_{\text{SERS}}^{(0)} \propto \left\| \frac{\mathbf{E}_{\text{loc}}(\omega_{\text{exc}})}{\mathbf{E}_0(\omega_{\text{exc}})} \right\|^4. \quad (1)$$

In equation (1), $\mathbf{E}_{\text{loc}}(\omega_{\text{exc}})$ and $\mathbf{E}_0(\omega_{\text{exc}})$ are the amplitudes of the local and incident electric fields, respectively, at the laser angular frequency ω_{exc} . Equation (1) implies that the laser excitation must be located within the resonance plasmon band in order to obtain a SERS spectrum. Unexpected from this equation, Fig. 2, spectrum B shows that a weak Raman spectrum is observed when the 647-nm laser line is polarized along the major axis of the particles (longitudinal polarization), thus prohibiting any plasmon excitation. This spectrum is unlikely to arise either from a polarizer misalignment or from any molecular enhancement since no SERS signal can be detected for infinitely long gold nanowires when the laser excitation is polarized parallel to the wire. In order to explain the presence of this weak SERS spectrum under longitudinal polarization, we consider a more realistic expression for the Raman gain:^{2,6,7,21}

$$G_{\text{SERS}}^{(1)} \propto \left\| \frac{\mathbf{E}_{\text{loc}}(\omega_{\text{exc}})}{\mathbf{E}_0(\omega_{\text{exc}})} \frac{\mathbf{E}_{\text{loc}}(\omega_{\text{RS}})}{\mathbf{E}_0(\omega_{\text{RS}})} \right\|^2 = g(\omega_{\text{exc}})g(\omega_{\text{RS}}). \quad (2)$$

In Eq. (2), $\mathbf{E}_{\text{loc}}(\omega_{\text{RS}})$ and $\mathbf{E}_0(\omega_{\text{RS}})$ are the local and incident electric field amplitudes, respectively, at the Raman angular frequency ω_{RS} . The overall gain is considered to be the product of a gain at the laser angular frequency $g(\omega_{\text{exc}})$ times a gain $g(\omega_{\text{RS}})$ at the Raman angular frequency. According to Eq. (2), the maximum of SERS signal is expected to occur when both the wavelength of the incident and the Raman scattered electromagnetic fields approach the LSP resonance. Weitz and co-workers have proposed a phenomenological relationship to evaluate the SERS enhancement,^{6,7}

$$I_{\text{SERS}} \propto \frac{c^2}{q^2 d^2} \frac{|\epsilon(\omega_{\text{exc}})|^2 A(\omega_{\text{exc}}) |\epsilon(\omega_{\text{RS}})|^2 A(\omega_{\text{RS}})}{\epsilon_2(\omega_{\text{exc}}) \omega_{\text{exc}} \epsilon_2(\omega_{\text{RS}}) \omega_{\text{RS}}}. \quad (3)$$

TABLE I. Wavelengths of the Raman lines (λ_{RS}) at 1610 and 1640 cm^{-1} and of the expected maximum enhancement (λ_{max}) for the three laser excitation lines used (λ_{exc}).

λ_{exc} (nm)	λ_{RS} (nm)		λ_{max} (nm)	
	1610 cm^{-1}	1640 cm^{-1}	1610 cm^{-1}	1640 cm^{-1}
633	704.6	706.1	668.7	669.5
647	722.2	723.8	684.6	685.5
676	758.6	760.3	717.3	718.2

In Eq. (3), $A(\omega) = (qd\omega\epsilon_2/c) \|\mathbf{E}_{\text{loc}}/\mathbf{E}_0\|^2$ is the absorbance, in which d is the effective film thickness, q is the volume fraction occupied by the particles on the array (particle coverage), c is the speed of light in vacuo, and ϵ_2 is the imaginary part of the particle dielectric function $\epsilon = \epsilon_1 + i\epsilon_2$. Equation (3) predicts that the maximum of SERS intensity occurs when the LSP resonance wavelength is equal to $\lambda_{\text{max}} = (\lambda_{\text{exc}} + \lambda_{\text{RS}})/2$, provided the absorbance is assumed to be of Lorentzian shape.¹⁰ Using silver island films as SERS substrates, the authors of Refs. 6 and 7 observed that, according to Eq. (2), the maximum of the SERS spectrum of nitrobenzoate was shifted towards long wavelengths with respect to the laser excitation line.⁶ More recently, Haunes, van Duyne and co-workers showed that, for silver particles obtained by nanosphere lithography, the SERS gain was maximized when the LSP wavelength λ_{LSP} was located between λ_{exc} and λ_{RS} .^{22,23} Thanks to very narrow size and shape distributions of the particles, the arrays used in this work exhibit sharp plasmon resonance, which enables us to experimentally demonstrate that SERS becomes maximum whenever the wavelength of particle plasmon resonance (λ_{LSP}) is positioned at precisely λ_{max} . In what follows, we clearly point out the advantages to use such arrays in SERS experiments.

Table I gives the wavelength (λ_{max}) at which the greatest SERS is expected to occur [see Eq. (3)] for the Stokes wavelengths (λ_{RS}) of the two investigated Raman bands excited by the three laser lines (λ_{exc}). Equation (3) enables us to propose a qualitative explanation for the residual SERS spectrum observed in Fig. 2, spectrum B for longitudinal polarization. $\|\mathbf{E}_{\text{loc}}/\mathbf{E}_0\|^2$ being proportional to the absorbance,¹¹ no SERS gain should be expected at $\lambda_{\text{exc}} = 647$ nm due to the lack of any particle plasmon excitation at this wavelength. According to Fig. 1, the Raman lines scattered at 722.2–723.8 nm can be enhanced by the weak particle plasmon excitation which serves as resonant amplifier of the Raman field.

In order to confirm this result, we fabricated an array in which the elongated gold particle size, shape, and spacing were chosen such that the maximum of the transverse plasmon band $\lambda_{\text{LSP}}^{\text{trans}}$ was located at the $\lambda_{\text{exc}} = 647$ nm krypton line and the longitudinal one $\lambda_{\text{LSP}}^{\text{long}}$ at $\lambda_{\text{max}} = 723$ nm when λ_{exc} is set at 676 nm. Figure 3 shows that the extinction spectrum of this array does exhibit two bands of almost equal extinction, located at 647 and 722 nm for the transverse and longitudinal polarizations, respectively.

The SERS spectrum of the BPE molecule excited at 647 nm is more intense under longitudinal polarization than under the transverse one, although the absorbance of the array is much stronger for transverse polarization (Fig. 4). This

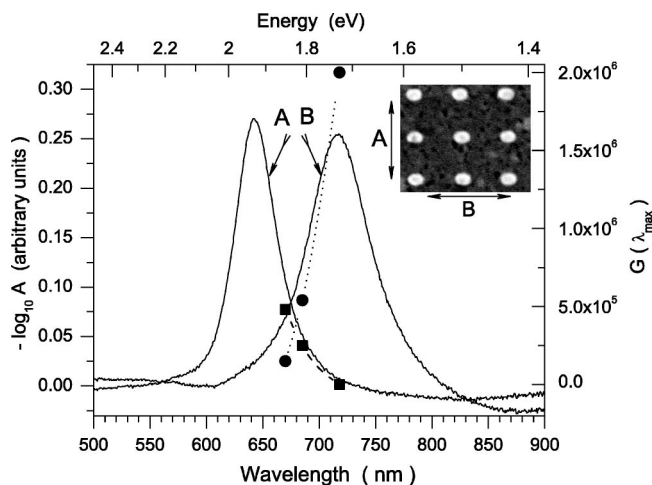


FIG. 3. Extinction spectrum of the array constituted of gold elongated particles; major and medium axes of 154 and 120 nm, respectively, are parallel to the substrate (particle aspect ratio $r=1.28$); the particle height is 40 nm and the interparticle spacing is 500 nm. Spectra are recorded by transmission under normal incidence in water, where "A" denotes the transverse polarization and "B" the longitudinal one. The full circles ●● and the squares ■■ denote the experimental Raman gain measured under laser excitation at 633, 646, and 676 nm under polarization along the particle major and medium axes, respectively. The Raman gains are plotted at λ_{\max} for each laser excitation wavelength λ_{exc} . Inset: scanning electronic image of the array (detail).

result is in agreement with our suggestion that the Raman gain should be maximum at $\lambda_{\max}=(\lambda_{\text{RS}}+\lambda_{\text{exc}})/2$ rather than at λ_{exc} . To confirm this observation, we performed the following experiments. From the SERS signal of the 1610 and 1640 cm^{-1} bands of BPE recorded at three laser excitation wavelengths ($\lambda_{\text{exc}}=633, 647,$ and 676 nm) under transverse and longitudinal polarizations, we determined the Raman enhancement factor per molecule, defined as previously.¹⁰ This Raman gain per molecule was found to be of the order of 10^5 – 10^6 with a standard deviation of about 10%, leading to relative variations of the gain which signify going from one excitation wavelength to the other. The SERS excitation pro-

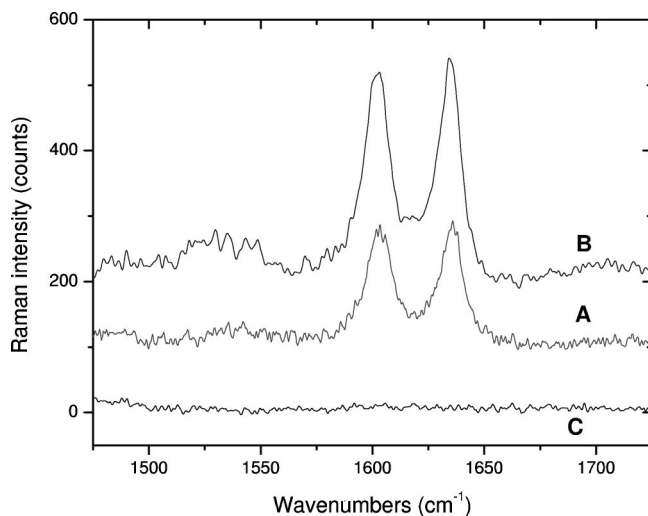


FIG. 4. SERS spectra of 5×10^{-4} M BPE aqueous solution on the grating of Fig. 3. Spectra A and B are recorded when the laser is polarized along the transverse and longitudinal LSP resonances, respectively, at $\lambda_{\text{exc}}=647$ nm; spectrum C is recorded out of the array (see caption of Fig. 2 for details).

file obtained by plotting this enhancement factor versus λ_{\max} can be compared to the extinction bands since the extinction spectra proceed mainly from absorption rather than from scattering according to discrete dipole approximation calculations.^{10,24} As shown in Fig. 3, the SERS excitation profiles for both polarizations follow remarkably the extinction band shapes. This result confirms our assignment of the residual SERS spectrum observed in Fig. 2, spectrum B to an enhancement of the Raman scattered field. There is no correlation between excitation profiles and plasmon bands when the Raman gain is positioned on the graph at λ_{exc} (not shown).

The sharp plasmon resonances resulting from the very narrow size and shape distributions of the lithographically designed particle arrays, point out clearly the advantages of using these arrays in SERS experiments compared to island films, which exhibit rather broad resonances. In our experiments on longitudinal LSP resonance, a Raman gain per molecule up to 2×10^6 can be obtained.

- ¹ *Surface-Enhanced Raman Scattering*, edited by R. K. Chang and T. E. Furtak (Plenum, New York, 1982); M. Moskovits, *Rev. Mod. Phys.* **57**, 783 (1985).
- ² M. Kerker, D. S. Wang, and H. Chew, *Appl. Opt.* **19**, 4159 (1980); P. K. Aravind, A. Nitzan, and H. Metiu, *Surf. Sci.* **110**, 189 (1981); S. L. McCall, P. M. Platzman, and P. A. Wolf, *Phys. Lett.* **77A**, 381 (1980); J. Gersten and A. Nitzan, *J. Chem. Phys.* **73**, 3023 (1980); R. Rupp, *Solid State Commun.* **39**, 903 (1981).
- ³ D. L. Jeanmaire and R. P. van Duyne, *J. Electroanal. Chem.* **84**, 1 (1977).
- ⁴ J. A. Creighton, C. G. Blatchford, and M. G. Albrecht, *J. Chem. Soc., Faraday Trans. 2* **75**, 790 (1980).
- ⁵ P. F. Liao, J. G. Bergman, D. S. Chemla, A. Wokaun, J. Melngailis, A. M. Hawryluk, and N. P. Economou, *Chem. Phys. Lett.* **82**, 355 (1981).
- ⁶ D. A. Weitz, S. Garoff, and T. J. Gramila, *Opt. Lett.* **7**, 168 (1982).
- ⁷ D. A. Weitz, S. Garoff, J. I. Gersten, and A. Nitzan, *J. Chem. Phys.* **78**, 5324 (1983).
- ⁸ R. G. Freeman, K. C. Garbar, K. J. Allison, R. M. Bright, J. A. Davis, A. P. Guthrie, M. B. Hommer, M. A. Jackson, P. C. Smith, D. G. Walker, and M. J. Natan, *Science* **267**, 1629 (1995).
- ⁹ N. Félidj, J. Aubard, G. Lévi, J. R. Krenn, G. Schider, A. Leitner, and F. R. Aussenegg, *Phys. Rev. B* **66**, 245407 (2002); L. Gunnarsson, E. J. Bjerneld, H. Xu, S. Petronis, B. Kasemo, and M. Käll, *Appl. Phys. Lett.* **78**, 802 (2001); M. Kahl and E. Voges, *Phys. Rev. B* **61**, 14078 (2000).
- ¹⁰ N. Félidj, J. Aubard, G. Lévi, J. R. Krenn, M. Salerno, G. Schider, B. Lamprecht, A. Leitner, and F. R. Aussenegg, *Phys. Rev. B* **65**, 075419 (2002).
- ¹¹ C. Y. Chen and E. Burstein, *Phys. Rev. Lett.* **45**, 1287 (1980).
- ¹² A. Otto, *J. Raman Spectrosc.* **22**, 743 (1991); F. R. Aussenegg and M. E. Lippitsch, *Chem. Phys. Lett.* **59**, 214 (1978).
- ¹³ A. J. Haes and R. P. Van Duyne, *J. Am. Chem. Soc.* **124**, 10596 (2002).
- ¹⁴ K. Kneipp, Y. Wang, H. Kneipp, L. T. Perelman, I. Itzkan, R. R. Dasari, and M. S. Feld, *Phys. Rev. Lett.* **78**, 1667 (1996).
- ¹⁵ J. A. Creighton, in *Surface-enhanced Raman-scattering*, edited by R. K. Chang and T. A. Furtak (Plenum, New York, 1982), p. 315.
- ¹⁶ S. J. Oldenburg, S. L. Westcott, R. D. Averitt, and N. J. Halas, *J. Chem. Phys.* **111**, 4729 (1999).
- ¹⁷ N. W. Gotschy, K. Vonmetz, A. Leitner, and F. R. Aussenegg, *Opt. Lett.* **21**, 1099 (1996).
- ¹⁸ B. Lamprecht, G. Schider, R. T. Lechner, H. Ditlbacher, J. R. Krenn, A. Leitner, and F. R. Aussenegg, *Phys. Rev. Lett.* **84**, 4721 (2000).
- ¹⁹ C. F. Bohren and D. R. Huffman, *Absorption and Scattering of Light by Small Particles* (Wiley, New York, 1983).
- ²⁰ U. Kreibig and M. Volner, *Optical Properties of Metal Clusters* (Springer, New York, 1995).
- ²¹ H.-G. Bingler, H. Bruner, A. Leitner, F. R. Aussenegg, and A. Wokaun, *Mol. Phys.* **85**, 587 (1995).
- ²² C. L. Haunes and R. P. Van Duyne, *Mater. Res. Soc. Symp. Proc.* **728**, S10.7.1 (2002).
- ²³ T. R. Jensen, M. L. Duval, K. L. Kelly, A. A. Lazarides, G. C. Schatz, and R. P. Van Duyne, *J. Phys. Chem. B* **103**, 9846 (1999).
- ²⁴ N. Félidj, J. Aubard, and G. Lévi, *J. Chem. Phys.* **111**, 1195 (1999).